P- and S-wave delineation of the Horseshoe Atoll, Diamond-M Field, Texas, USA

Carlos Russian, Roderick Perez, Kurt Marfurt, Oswaldo Davogustto, *and* Hani Alzahrani, *University of Oklahoma*
Alison Small, *Parallel Petroleum LLC*

This paper presents an applied workflow for displaying seismic multi-attributes and integrating the results into the interpretation of a carbonate reservoir. This analysis compares the processed volume of the conventional P-wave data (PP) with the S-wave data (SH-SH) over the same extended area to improve understanding of the morphology of the reef "build-up" structure within the Canyon Reef Formation. The final goal is to identify bypassed compartments in the reservoir.

The comparison focuses on attribute volumes calculated for both P and S data using variance-based coherence and volumetric curvature (including the shape index). Analysis of the conventional P-wave survey and the S-wave survey includes angle stack gathers (0–10°, 10–20°, 20–30°, 30–40°, and 40–50°), and a full stack gather. An interpretation of key horizons from previous work plus access to dipole sonic logs and well tops provided an abundance of information to better calibrate the interpretation of the reef and its geomorphology.

Geologic background

The Horseshoe Atoll is an arcuate chain of reef mounds of mixed types of bioclastic debris that accumulated in the interior part of the developing Midland Basin during Late Paleozoic time (Vest, 1970). The atoll complex consists of three bioclastic carbonate units: the Strawn, Canyon, and Cisco formations, in ascending stratigraphic order. Core and log data indicate the Cisco has a greater biogenic build-up, erosion, and karst. The Canyon and Strawn formations are more horizontally bedded. These heterogeneous carbonate units are separated by locally correlative shale beds (Galloway et al., 1983).

Figure 1 shows the location of the Diamond-M Field on the Scurry Reef Trend in Scurry County, Texas (Walker, 1995). It is part of the larger Pennsylvanian-age Horseshoe Atoll Reef Complex—massive carbonate units separated by locally correlative shale beds. This paper will focus on the Canyon Reef Formation of the Upper Pennsylvanian age.

The porosity signature from existing well data shows that the Canyon Reef reservoirs in this area are highly compartmentalized, which we interpret to be due to the rapid lateral variation associated with the varying organization of the reef as it was developing.

Data and methodology

The Diamond-M survey offers a chance to analyze differences in attribute response between PP-wave data and SS-wave data. PP refers to data resulting from a compressional-wave source recorded on vertical component receivers. SS refers to data from shear-wave sources (vibrating inline and perpendicular to the source line) with receivers inline and

Figure 1. *Late Paleozoic paleo-geographic map of west Texas. Red star denotes Diamond-M Field (Walker, 1995).*

perpendicular to the receiver line. At near angles, PP images are primarily sensitive to changes in P-wave impedance, while SS images are primarily sensitive to changes in S-wave impedance. The expectation is that differences in reflectivity between PP and SS data may lead to differences in stratigraphic resolution and structural clarity. Together, they can help estimate lithology, potentially differentiating between various carbonate facies associated with reef complexes that have undergone diagenetic alteration. The seismic data on this project can be divided into four subsets: PP full stack, SS full stack, PP angle stacks, and SS angle stacks. In this project, "full stack" means the sum of partial angle stacks corresponding to 15, 25, and 35°. Differences in reflection coefficients with incident angle may lead to better delineation of stratigraphic features on angle stacks.

The first step in interpretation of joint PP and SS data volumes is to tie the wells and generate corresponding time structure maps to register the two volumes. The best horizon to use is the strong shale/carbonate reflector (yellow pick in Figure 2), corresponding to the top of the Canyon Reef Formation. Following workflows developed to delineate pinnacle reefs in Canada (e.g., Chopra and Marfurt, 2007), we chose time slices at 0.935 s on the PP and 1.871 s on the SS volumes that cut the reef just below the top of the Canyon Reef Formation. The Canyon Reef Formation corresponds to the
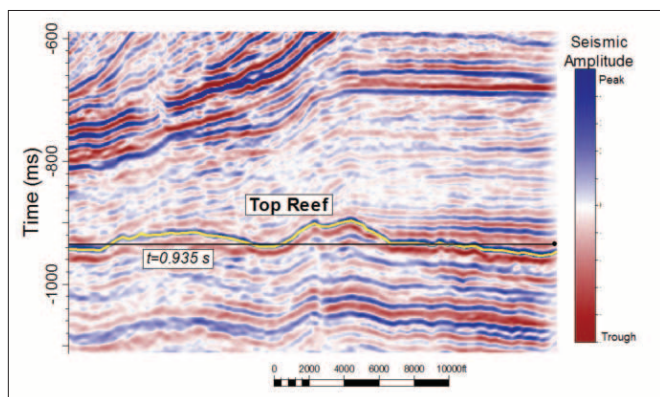
Figure 2. Seismic cross section corresponding to the PP full stack volume. The yellow horizon indicates the top of the Canyon Reef Formation. The black line indicates the location of the time slice at 0.935 s.

latest stage of deposition in a carbonate sequence.

We use seismic attributes to delineate the edge of the reef build-up and internal architectural elements. After 50 years of production (including water flood), the operators are still finding small, untapped compartments as they infill to 20-acre spacing. High-porosity zones are limited, and some producing zones lie outside the reef, suggesting production from talus slopes toward the reef's flanks. There are baffles and barriers between them laterally as well as tight zones that separate them in a vertical and lateral sense. Ideally, attributes may allow us to see boundaries between adjacent, noncommunicating reservoir compartments with different pressures and oil-water contacts. Once this pattern is recognized, we may be able to identify reservoir compartments that have not yet been drilled.

Multi-attribute analysis

Seismic attributes enhance subtle amplitude, frequency, phase, and morphological components of conventional 3D data that may otherwise be difficult to see. One of the more successful interpretation workflows is to use mathematically independent attributes coupled through some underlying geologic feature of interest. By combining multiple attributes into a single image, we can visually "cluster" these independent attributes to reduce the ambiguity in our interpretation.

In this paper, we show the interpretive value of what we believe to be an underutilized attribute, the volumetric shape index. Some of the earliest applications of the shape index were in the quantification of geographic terrains to define drainage basins and microclimates. Mathematically, the shape index combines the most-positive and most-negative principal curvatures, k_1 and k_2. By definition, $k_1 \geq k_2$. Thus, if both k_1 and k_2 are less than zero, we have a bowl; if both are greater than zero, we have a dome; and if both are equal to zero, we have a plane.

Shape attributes are a combination of the shape index and the curvedness attributes, where curvedness describes the magnitude of the curvature independent of its shape. The result is the image in Figure 3. Notice how the time contours of the seismic interpretation correspond neatly to volumetrically
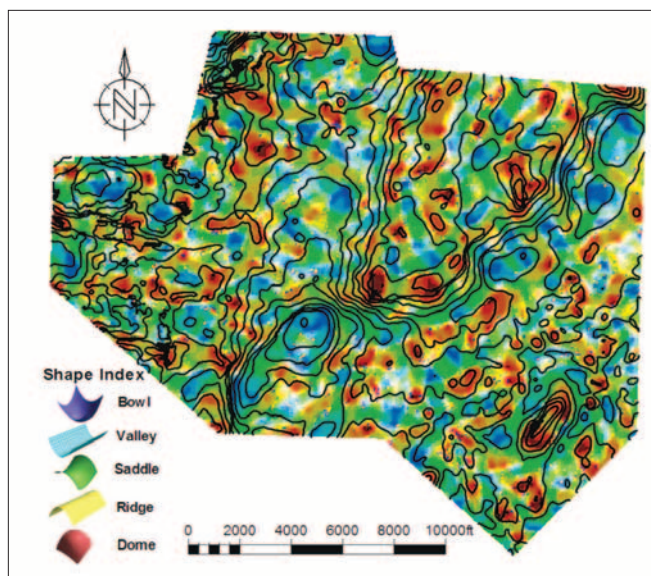

Figure 3. Volumetric shape index attribute extracted along the Canyon Reef horizon. Contour lines correspond to time contours of the seismic interpretation.
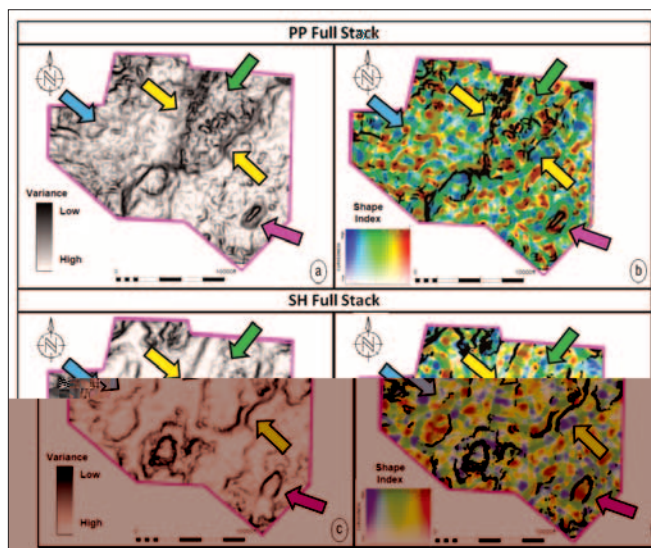

Figure 4. Comparison of approximately registered time slices near the top Canyon Reef through (a) variance-based coherence and (b) shape index computed from the PP volume at 0.935 s corendered with coherence and (c) variance-based coherence and (d) shape index computed from the SS volume at 1.871 s corendered with coherence.

computed shape indices along the top of the reef.

PP and SH full stack multi-attribute analysis

It is expected that the lithology contrast between the reef and its surrounding lithology (mostly shale) will have a direct impact on the waveform such that the edges of the reef will be highlighted. When comparing the results of the PP and SH coherence attributes, note that the edges of the reef are better resolved in the SH volume than in the PP volume (Figure 4). In contrast, the PP volume better delineates smaller reef structures generally referred to as "patch" reefs (green arrow). Also note the smaller reef build-up in the southeastern area
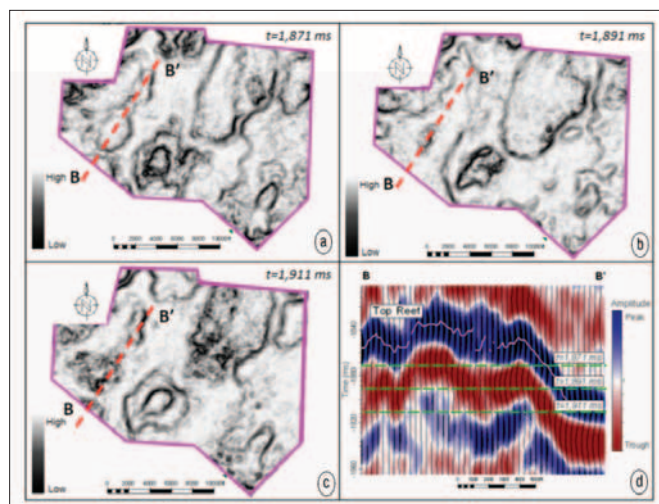
Figure 5. *Different stages of the reef formation seen on time slices through the SH variance volume at (a) 1.871 s (b) 1.891 s, and (c) 1.911 s. Red dashed line indicates the location of the cross section B-B¹ in (d).*

of the survey (magenta arrow). SH variance shows how the reef is divided into two smaller reefs (blue arrow) while the corresponding PP variance fails to delineate this subtle but important feature.

Figure 5 displays three time slices through variance computed from the SH amplitude volume, showing changes in position of the edges of the reef, that reveal different episodes in the formation of the reef body. At 1.871 s (Figure 5a), we see the latest stage of deposition of the Canyon Reef Formation. At 1.891 s (Figure 5b), corresponding to the middle stage of the reef formation, we see a broader reef. Finally, at 1.911 s (Figure 5c), we see an earlier stage of deposition nearer the base of the reef. The cross section B-B' (dashed line) corresponds with the vertical section in Figure 5d.

PP angle stack multi-attribute analysis

Both PP and SS reflections vary with angle and provide further leverage to estimate changes in lithology. In the present study, the differences of angle of incidence with respect to offset/angle further enhance the delineation of the reef as seen by time slices at the Canyon Reef Formation level through attribute volumes computed from angle-limited migrated volumes.

Figure 6a is a time slice at 0.935 s through the variance computed from the 15° PP angle stack volume. Note that the edges of the reef (yellow arrows) have been resolved and smaller carbonate features within the main reef denoted by the green arrow can be resolved. The left-most reef structure (cyan arrow) is difficult to distinguish, but can be identified with the help of conventional time-structure maps. A smaller reef structure is indicated by the magenta arrow and a suite of circular patch reefs are highlighted by white arrows. This interpretation is consistent with dome-to-ridge structures seen on the shape index volume.

Figure 6c is time slice at the same level through variance computed from the 25° PP angle stack. Yellow arrows indicate
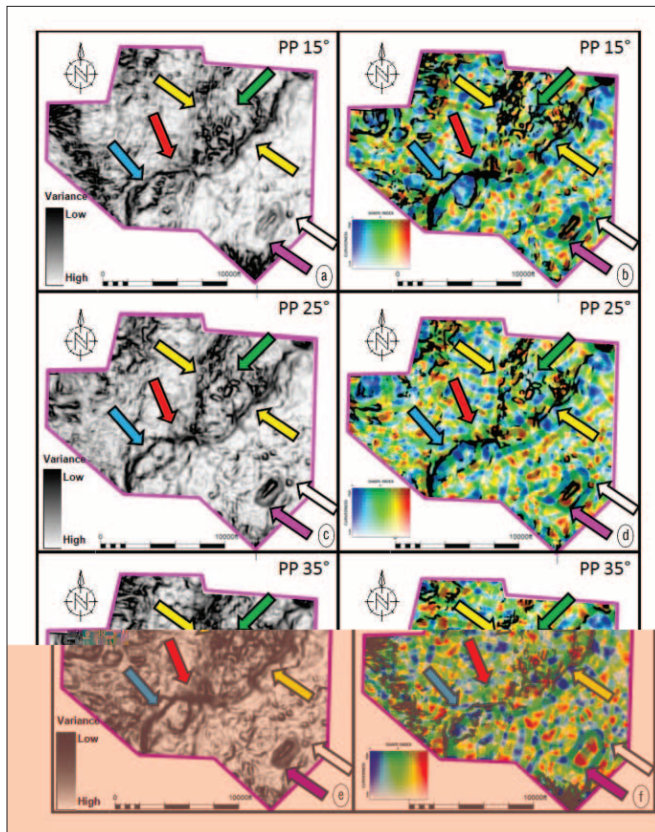
Figure 6. *Variance-based coherence index time slices at 0.935 s through angle stacks (a) PP15, (c) PP25, and (e) PP35, and volumetric shape index time slices corendered with coherence through angle stacks (b) PP15, (d) PP25, and (f) PP35. Arrows explained in the text.*

areas of improved illumination of the reef edge, with some incoherent events in the inner portion of the central reef (green arrow). To the southeast, a well-defined build-up (magenta arrow) exhibits well-resolved circular patterns (white arrow). Figure 6e is a time slice at the same level through the 35° PP angle stack. At these higher incidence angles, the features are not as well resolved as in the more vertical illumination as seen by the edges (yellow arrow), inner circular features (green arrow), small build-up of reef (magenta), and circular patch reefs (white arrow). A similar case has less geologic delineation when comparing shape index as the angle increases. Blending coherence with shape index (Figures 6b, 6d, 6f) leads to an optimal interpretation of the morphology of the reefs in terms of its shape (bowl, valley, saddle, ridge, and dome). Cyan and red arrows indicate areas where we are unable to delineate the western-most portion of the reef or the depression between the reef structures.

Rose diagrams

More conventional display and qualification of lineaments can be obtained from rose diagrams which can be generated for any gridded-square area defined with an *n*-inline by *m*-crossline analysis window, for each horizontal time slice. Within each analysis window, each pixel is binned into rose petals according to its azimuth (ψ_{min}), weighted by its
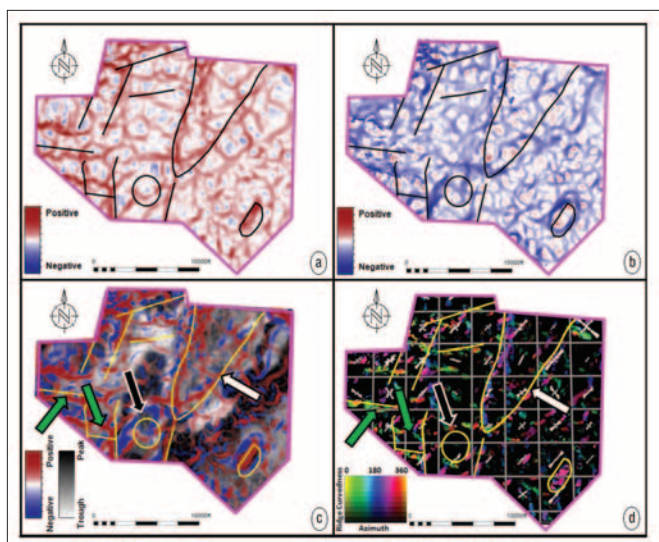
Figure 7. *Time slices at 0.935 s through (a) most-positive principal curvature, k_1, (b) most-negative principal curvature, k_2, (c) corendered most-positive and most-negative principal curvatures with variance, and (d) rose diagrams showing the trend of ridges computed from the full-stack PP volume.*

Figure 8. *Time slices at 1.871 s through (a) most-positive principal curvature, k_1, (b) most-negative principal curvature, k_2, (c) corendered most-positive and most-negative principal curvatures with variance, and (d) rose diagrams showing the trend of ridges computed from the full-stack SS volume.*
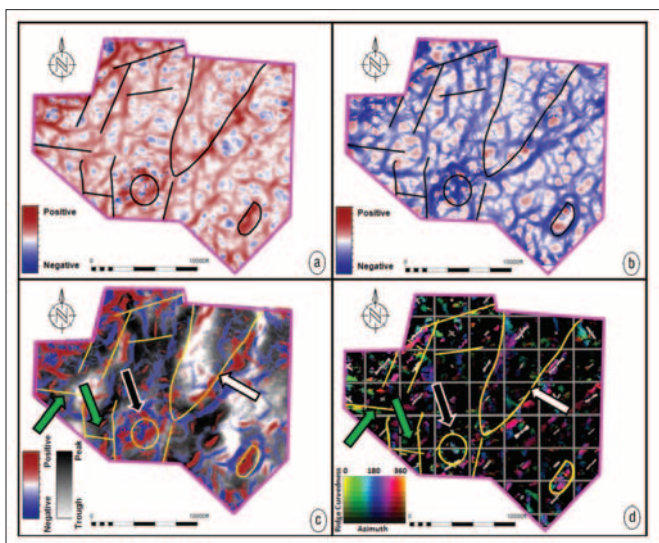
threshold-clipped ridge or valley components of curvedness, then summed and scaled into rose diagrams. The process is repeated for the whole data volume. After that, the rose diagrams are mapped to a rose volume which is equivalent to the data volume, and centered in the analysis window, at the same location as in the input data volume. Rose diagrams, computed for the whole lineament volume (corresponding to the seismic volume), yield intensity and orientation of lineaments.

Thus rose diagrams are generated from two significant attributes, namely, the azimuth of minimum curvature and as stated above another attribute that would have a good mea-

sure of the shape of the features. This attribute could be the valley attribute or the ridge attribute. For this study, we prefer ridge curvedness because it is most likely associated with the geology of the reef build-ups; this does not mean that valley shape attribute would not derive interesting results, but we did not consider it in this study.

Other attributes, such as positive and negative curvature, estimated lineaments corresponding with the edges of the reef and to inner structures within the reef build-up. These lineaments suggest possible relation to fractures and bending of the reef (Figure 7 and Figure 8).

Figure 7 shows the results of PP data on a time slice at 0.935 s just below the top of the Canyon Reef Formation through (a) most-positive and (b) most-negative curvature volumes. We used transparency to show anomalous features on top of the seismic amplitude time slice (Figure 7c). In the blended image of most-positive and most-negative curvature (Figure 7c), in addition to edges of the reef we observe chaotic behavior on curvatures related to a possible reef talus slope on the eastern flank of the central reef (white arrow) correlating to a high-amplitude response on the amplitude map. Figure 8 shows a similar comparison for SS data.

A 2D multi-attribute display was generated to combine the ridge curvedness with minimum curvature azimuth, overlaid with volumetric rose diagrams (Figure 7d). This composite display helps visualizing lineaments which correspond to the reef's edges and potentially indicate inner-structure compartmentalization of the reef. The minimum curvature azimuth represents the strike direction of a curved feature, with azimuth ranging from –90 to 90°, so it is represented by a cyclic color range, in this case as hue on a 2D color map. Ridge curvedness (c_r) represents the degree of curvedness of ridge-like features; where c_r is small the feature at the analysis location is flatter and where c_r is large, the feature is more likely to be ridge-curved. We represent this curvedness with lighter colors on a 2D map.

Although the lineaments from the PP and SS data volumes are similar, detailed comparison suggests that lineaments differ in some areas. In Figure 8, the most westerly lineaments (green arrows) cannot be detected as clearly as in the previous PP data volume, and a central valley (black arrow) is not apparent. On the other hand, the SS data set improves interpretation of the central "main" reef because the edges are better resolved and defined. Subsequently constructed rose diagrams (Figure 8d) better define lineaments associated with the central reef.

Conclusions

Multi-attribute displays reveal subtle but important features that could have significant importance for reservoir modeling and understanding reservoir compartmentalization. With the use of a variety of attributes over the Diamond-M survey, it was possible to better define the edges of the reef and as inner structures interpreted as smaller patch reefs. We think that integrated interpretation of several different attributes was necessary to understand the morphology of the reef build-up structure within the Canyon Reef Formation. The workflow

presented in this paper helped in identifying by-passed compartments in this fractured reservoir, hence prioritizing areas for drilling and in planning water flood and CO_2 injection locations.

The variance-based coherence attribute has defined in an optimum way the geomorphology of the reef. The PP volume apparently better defines the inner reef incoherent events while the SS volume estimates of coherence best resolved the edges of the reef in general. In the case of angle stacks, the edges of the central reef can be better delineated in the PP 25° angle stack as well at the southeast build-up reef (magenta arrow in all figures). However, the western-most portion of the reef and depression are best characterized on the SS 15° angle stack. The shape index attribute is a powerful and complementary interpretation tool, which when calibrated with structure maps, delineates dome-ridge-saddle-valley-bowl, thus prioritizing areas of interest for drilling. The ridge curvedness that better correlated with reef build-up structures was the reason identifying this particular feature in shape index results lead to areas with potential hydrocarbon accumulation.

There are several items to point out that could explain the reasons why some features are better resolved in the PP data set or in the SS data set:

1) More severe attenuation of shear waves than compressional waves propagating through the media.
2) Diverse processing workflows used for each volume (PP and SS data sets).
3) Higher signal-to-noise ratio on the PP survey than in the SS survey.
4) Differences in frequency content (the PP data set being double the SS data set in frequency content).
5) The difference in acoustic impedance between the P-wave and the S-wave data. *TLE*

References

Chopra, S. and K. J. Marfurt, 2007, Seismic attributes for prospect identification and reservoir characterization: SEG.

Galloway, W. E., T. E. Ewing, C. M. Garrett, N. Tyler, and D. G. Bebout, 1983, Atlas of major Texas oil reservoirs: Bureau of Economic Geology.

Vest, E. L., 1970, Oil fields of Pennsylvanian-Permian Horseshoe atoll, west Texas in Geology of giant petroleum fields: American Association of Petroleum Geologists Special Volume 14, 185–203.

Walker, D. A., J. Golonka, A. M. Reid, and S. T. Reid, 1991, The effects of late Paleozoic paleolatitude and paleogeography on carbonate sedimentation in the Midland Basin, Texas; Permian Basin plays: Society of Economic Paleontologists and Mineralogists, Permian Basin Chapter, Tomorrow's Technology Today, 141–162.

Corresponding author: roderickperez@ou.edu